

# **Seismic parameter design for reservoir monitoring, Brooks, Alberta**

Davood Nowroozi and Donald C. Lawton

## **ABSTRACT**

The main objective of this paper is to evaluate a 3D-3C seismic survey in order to make possible 4D and reservoir studies to monitor CO<sub>2</sub> injection and map the underground layers and structures. A porous and permeable formation (the Medicine Hat sandstone) as a reservoir with reliable cap (low permeability) that is the Colorado shale are injection targets for CO<sub>2</sub> sequestration and also for the seismic survey design. The project area is a field located southwest of Brooks, Alberta. The first part is data gathering and analysis results for velocity functions and desired frequency content of targets (shallow and deep) and the second part is the parameter estimation for preventing spatial aliasing and suitable resolution for the reservoir study. For the bin size and migration aperture estimation, constant and linear velocity methods were considered. Finally, two options are introduced and their attributes (fold map for PP and PS data with different offset, offset and azimuth distribution) are compared.

## **INTRODUCTION**

The project area is located southwest of Brooks city, west of the Newell Lake (Fig.1). This field was selected due to CO<sub>2</sub> sequestration test then observing reservoir behaviour and geophysical responses during and after the injection process.

The proper designing parameters can guarantee success of seismic studies from processing to interpretation and 4D reservoir studies. Current paper has two parts, the first is background study for gathering required information for designing stage and designing parameters. The next part will introduce two option and compares designing attributes for them.

## **BACKGROUND INFORMATION**

For a regular onshore seismic designing project, seismic parameters are calculated and selected by influence of:

1. Geology of area (surface , subsurface and structural condition as layers dip angle)
2. Terrain conditions (topographic, permit ...)
3. Frequency contents (Max and dominant) in the targets and required resolution
4. Velocity and velocity as a function of depth
5. Objective of acquisition (image, reservoir study,...) and main targets (the shallowest and deepest)

6. Full fold Image zone for structural or reservoir studies to estimate acquisition boundary and area by calculating migration aperture and fold taper



FIG.1. Satellite image of Brook's study area (Google Earth).

7. Seismic data (row shots for a better frequency analysis and sections for interpretation and evaluation and both for controlling quality of data and problems)
8. Technical part and existence technology (recording system)
9. Financial conditions and limitations

The next part introduces the required information for the design.

## GEOLOGY

The design area is in the southern Alberta basin. 2D and 3D seismic data demonstrate flat subsurface in the target zone. Table 1 demonstrates formations and objective depth for seismic designing target.(according to well data in the location 00/07-22-017-16W4/0 or (E420422, N5588774 UTM)). Main target is Medicine Hat sandstone that is in the 450-710 m depth.

Depth (m)	Formation Top	Period	
189.74	Top of log data	Upper	Cretaceous
296.5	PAKOWKI		
357	MILK RIVER		
441.5	COLORADO SHALE		
478.5	MEDICIN HAT SANDSTONE		
711	SECOND WHITE SPECKLED SHASLE		
785	FISH SCALES	Lower	
826	BOW ISLAND		
938.5	MANNVILLE		
1036	GLAUCONITIC		
1059	OSTRACOD		

Target

Table 1. Target zone for seismic designing, according to well (CVE 4A COUNTLESS 4-36-17-16 ) data , coordinate (E420422, N5588774 UTM).

### Frequency content

For a flawless bin size estimation and designing, max and dominant frequency on the target formations should be analyzed from old VSP and 2D, 3D seismic data. Relation between frequency (f), deep angle ( $\theta$ ), interval velocity (V) and bin size (B) for unaliased data is:

$$B = V_{int} / (4f_{max} \sin\theta) \quad (\text{Eq.1.})$$

There are many old 2D and 3D seismic surveys in area. The best way is analyzing frequency content of this data (before filtering) if row shots are not accessible. According to frequency content analysis, dominant frequency for the target formations are between 30-70 Hz and for the max frequency it is 80 Hz.

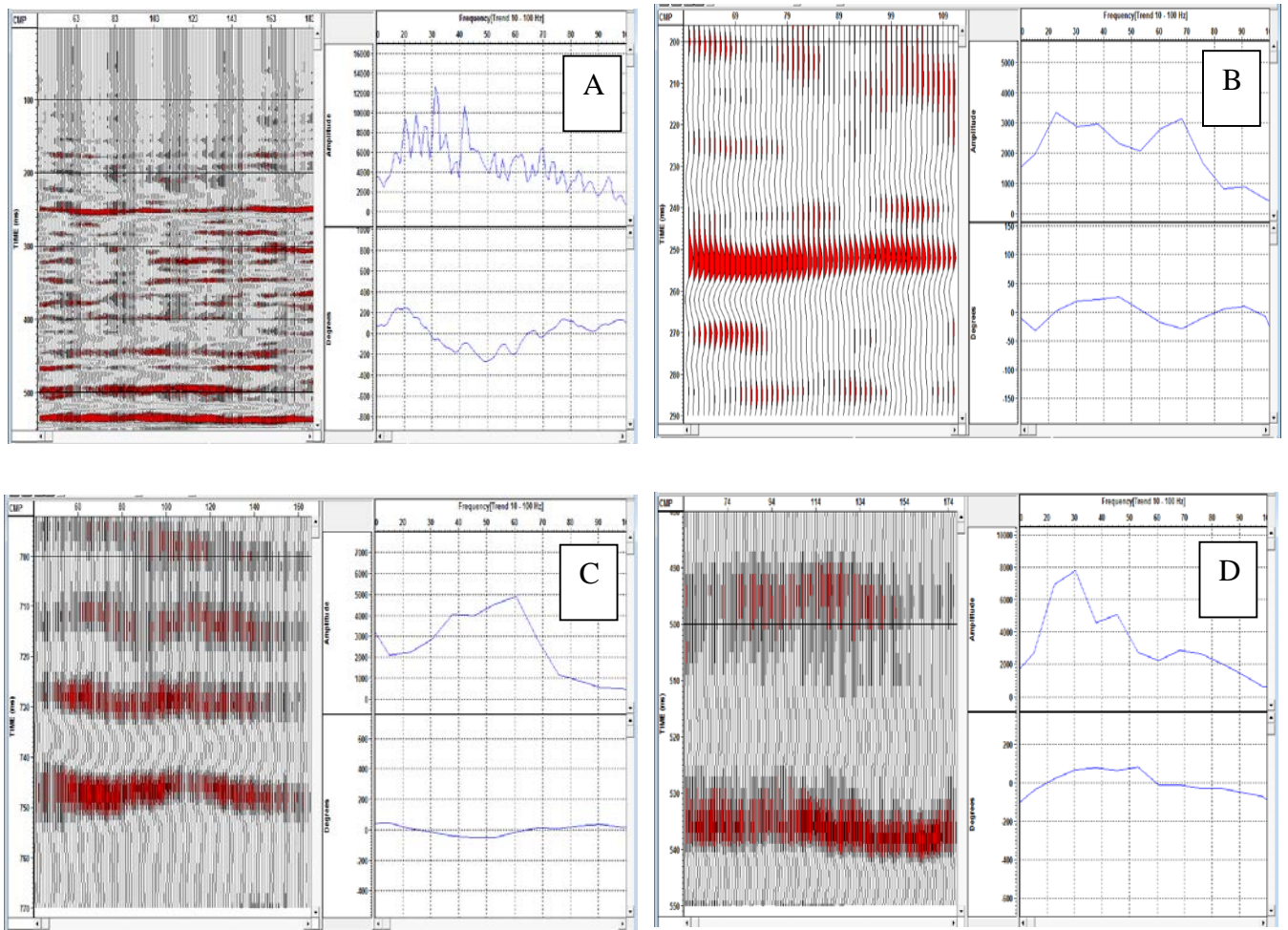


FIG.2. Frequency analysis on the whole seismic section from 0-550 ms (A), The shallowest target (B) and the deepest targets (C,D)

## Velocity-depth

Well log data is a liable source for compressional and shear wave velocity profile, for shear wave velocity that is not available in the well log data here, there are some approaches as mudruck approximation or calculating  $V_s$  from  $V_p$  and Poisson's ratio. Here simply  $V_s$  is considered half of  $V_p$ . For bin size and migration aperture estimation, it is possible to use constant and linear velocity. Using linear velocity in the calculations can optimize cost, especially it decreases migration aperture and acquisition area.

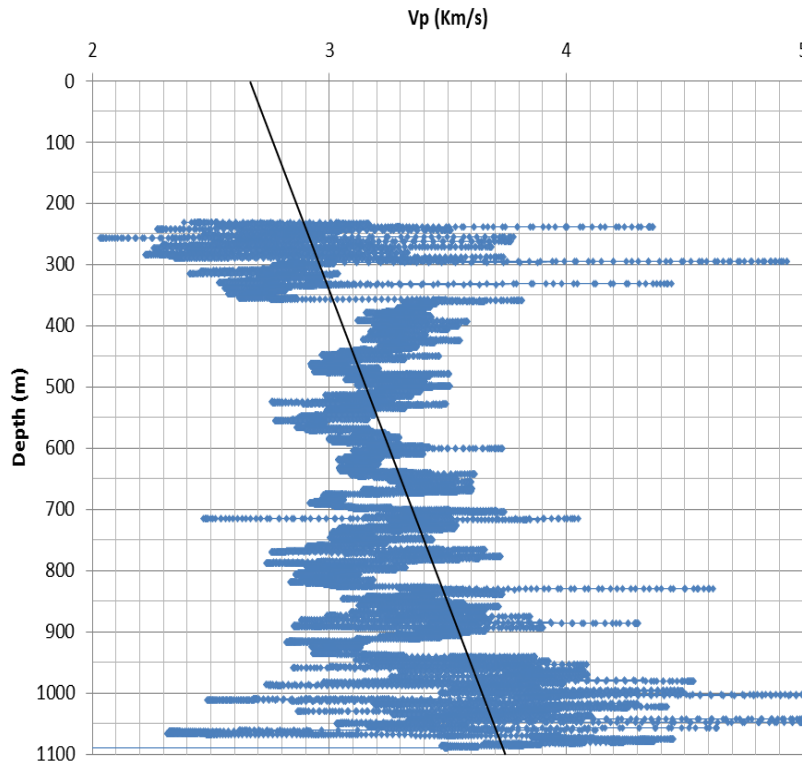


FIG.3. As mentioned, linear function for velocity can be used in the bin size's and migration aperture's calculation. Velocity function for Brook's project regards to well log data (CVE 7B countess 7-22-17-16) is:  $V=V_0+kz=2650+z$ .

### BIN SIZE

Appropriate Bin size can guaranteed a data set without aliasing problem, small bin size can prevent to acquire unaliased data, but also can decrease S/N ratio (Cordsen et al., 2000). This paper do not pay to spatial aliasing concept and here we directly use anti-aliasing Bin size formula (eq.1) for the constant velocity.

The project area is situated in flat plain, and also subsurface layers have a gentle dip angle less than 2 degree. For a flat subsurface condition, dip angle that is used in formula is  $\theta = \text{Max}(30, \text{real dip angle})$  (Vermeer, 2002). It is to make possible for gathering all diffraction events.

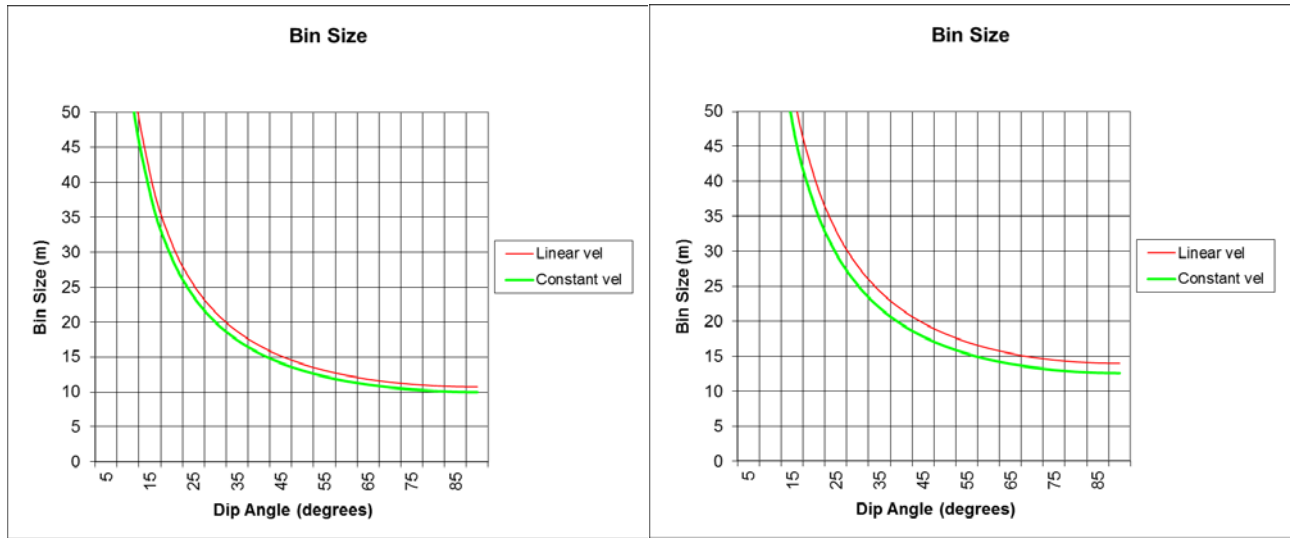


FIG.4. Bin size for the shallow target with 80Hz max frequency (left diagram) and for the deep target with 65Hz (right diagram).

### BOX SIZE AND GEOMETRY

The box size and geometry can bring the LMOS (largest minimum offsets) concept to the designing. As mentioned, the target depth is from 300-700 m, and for acquiring data with suitable fold on the target depth, LMOS should be equal or smaller than first target depth, because it make a no data zone equal to LMOS. Other problem that increases fold in the shallow depth is NMO stretch and mute so for the project, and in the parameter designing should be considered (FIG.5).

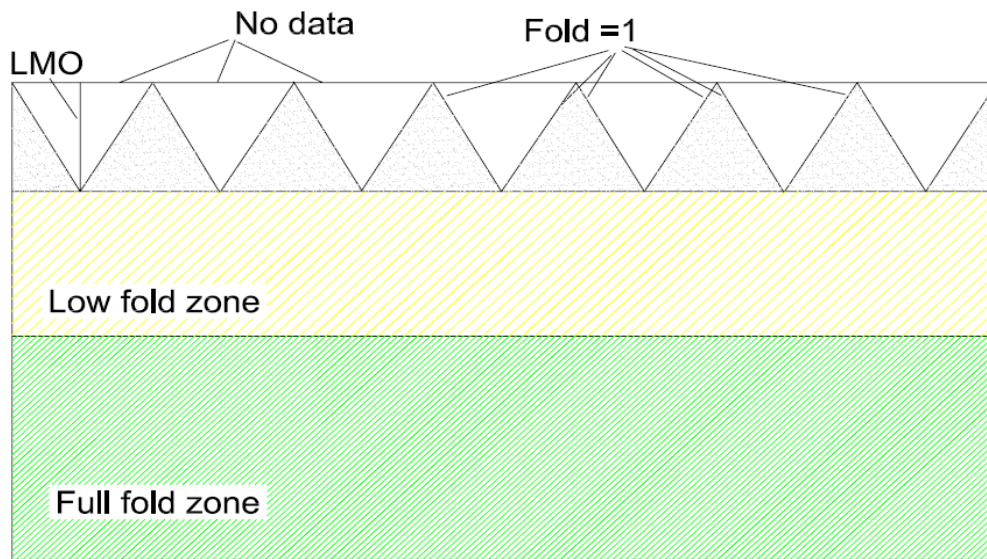


FIG.5. Influence of mute function (in low data zone) on calculating maximum offset and effect of LMOS on no data zone. The stretch factor (SF) defines the maximum offset, the small SF will make less fold in the survey and consequently data will be expensive and the larger one will decrease resolution (Vermeer, 2002).

For the reservoir and AVO studies, a symmetric geometry for the box and the patch with aspect ratio ~1 is selected.

### PATCH SIZE AND MAXIMUM OFFSET

Now XMax or LMO and bin size are known, other parameter for the template size calculation is the maximum offset (XMax).

The deepest layer or final target has main rule on XMax calculation, source power (charge in explosive and force in vibrator) and record length. There is a rule of thumb about relation between maximum offset and the deepest target (Stone, 1996):

$$X_{Max} \geq \text{Deepest target} \quad (\text{Eq.2.})$$

And for a flat layer, Maximum offset can be defined as:

$$X_{Max} = \frac{1}{2} Z \left( \frac{V+V_s}{V-V_s} \right)^{\frac{1}{2}} \quad (\text{Eq.3.})$$

Where V is rms velocity to the target and Vs is velocity of the surface layer.

Other parameters as direct wave interference, refracted wave interference, deep horizon critical reflection offset, Max NMO stretch are important for the maximum offset's calculation and selection (Cordsen et al., 2000).

### MIGRATION APERTURE

For calculating migration aperture in this project, linear and constant velocity were used. Fig.6 indicates range of migration aperture for different dip angles. The conservative designers usually use 15 or even 30 degree when subsurface layers are flat.

	Migration distance with linear velocity function											Xv
	Migration distance with a constant velocity function											Xc
□	15	20	25	30	35	40	45	50	60	70	75	90
Xv	167	225	287	351	420	495	577	668	884	9508	1340	2049
Xc	188	255	326	404	490	587	700	834	1212	1923	2612	>89 degrees

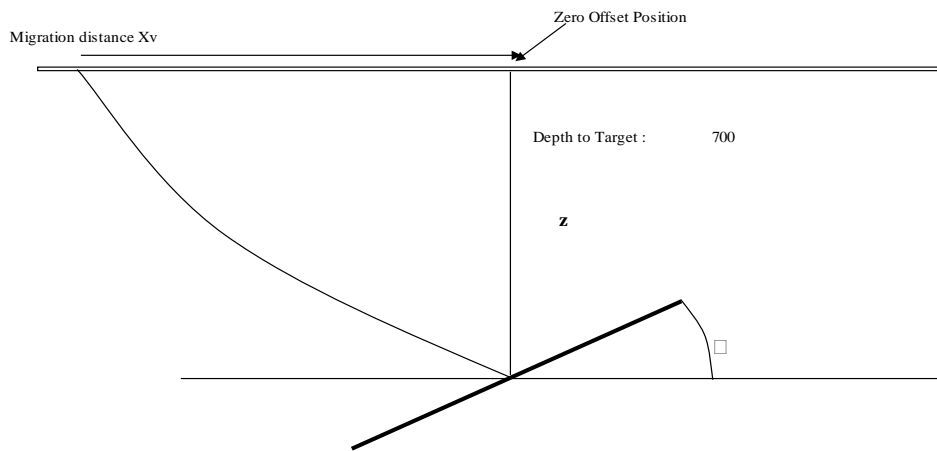


FIG.6. Migration aperture calculation by constant and linear velocity.

## SEISMIC MODELLING

Well log data for velocity and density with seismic sections helps to make 1D and 2D synthetic seismogram precisely. Figures 7 and 8 indicate PP wave section in time and depth and fig.9 is a time section of PS wave data. For the model, spread length is 700m and group interval is 10m.

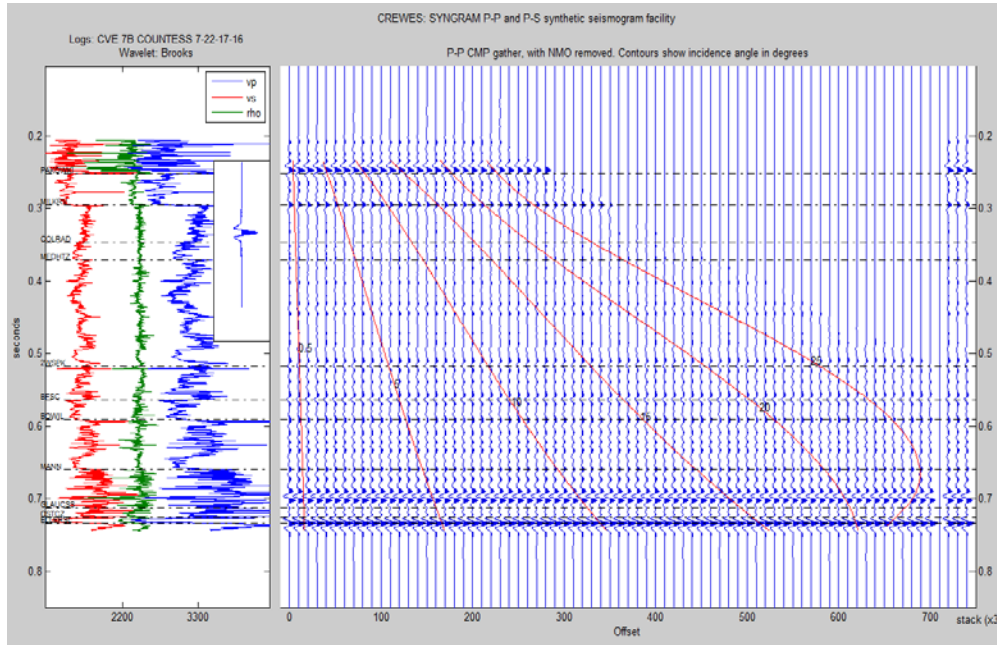


FIG.7. Synthetic seismogram (in time), target zone is 250 to 520 ms. (NMO removed)

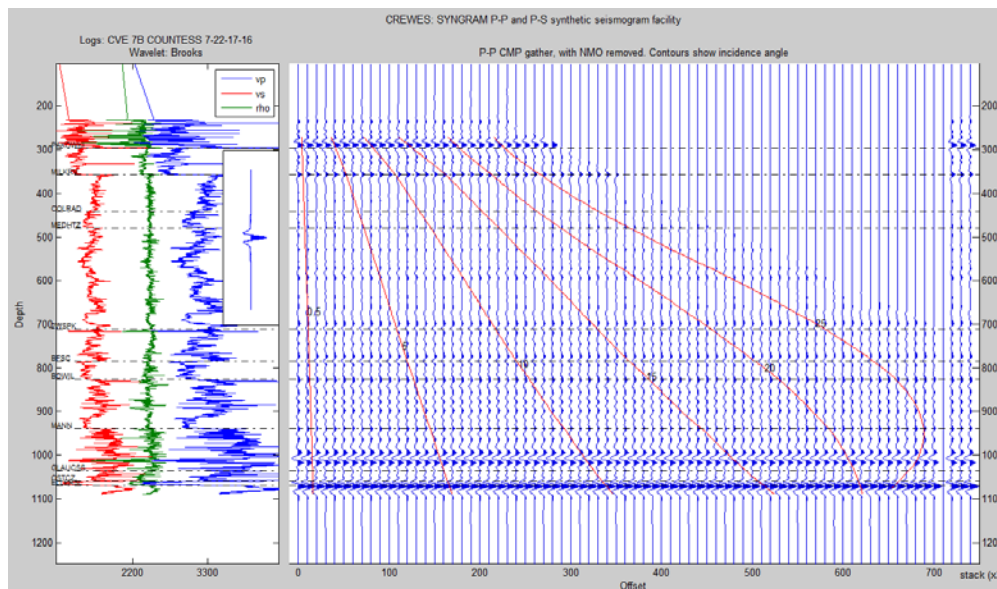


FIG.8. Synthetic seismogram for PP wave in depth, targets are in 300 to 700 m depth (NMO removed)



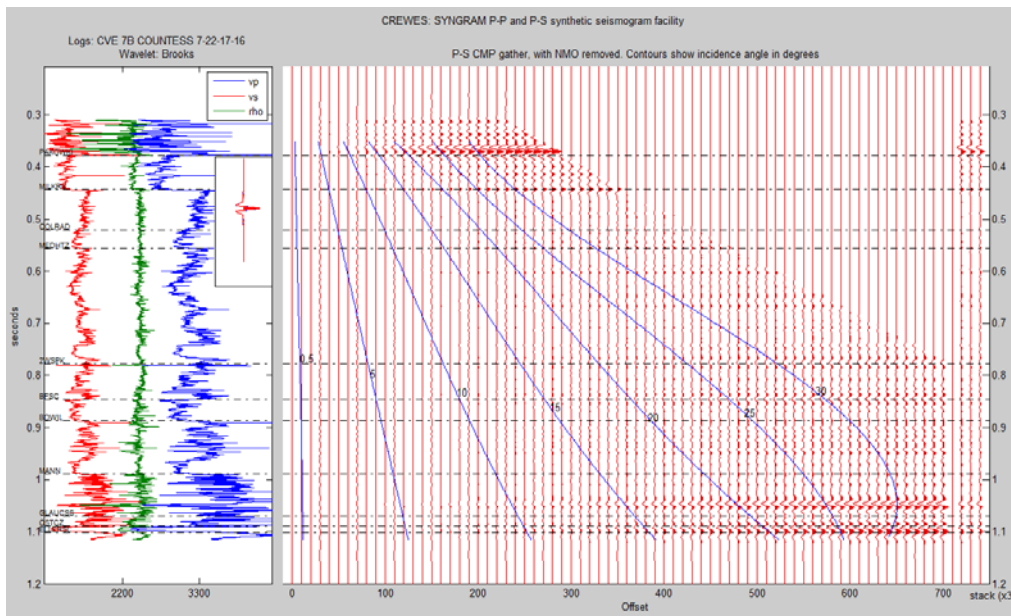


FIG.9. Synthetic seismogram (in time, NMO removed) for S wave; group interval=10 m and Max offset=700 m

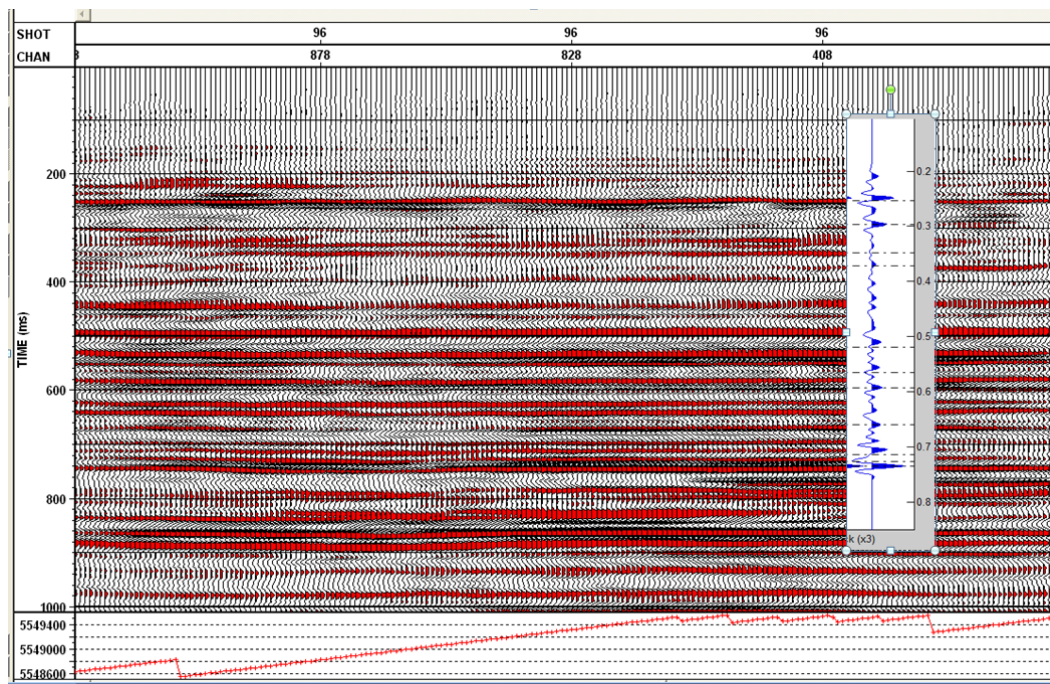


FIG.10. Comparing a real seismic section from the project area with the synthetic seismogram

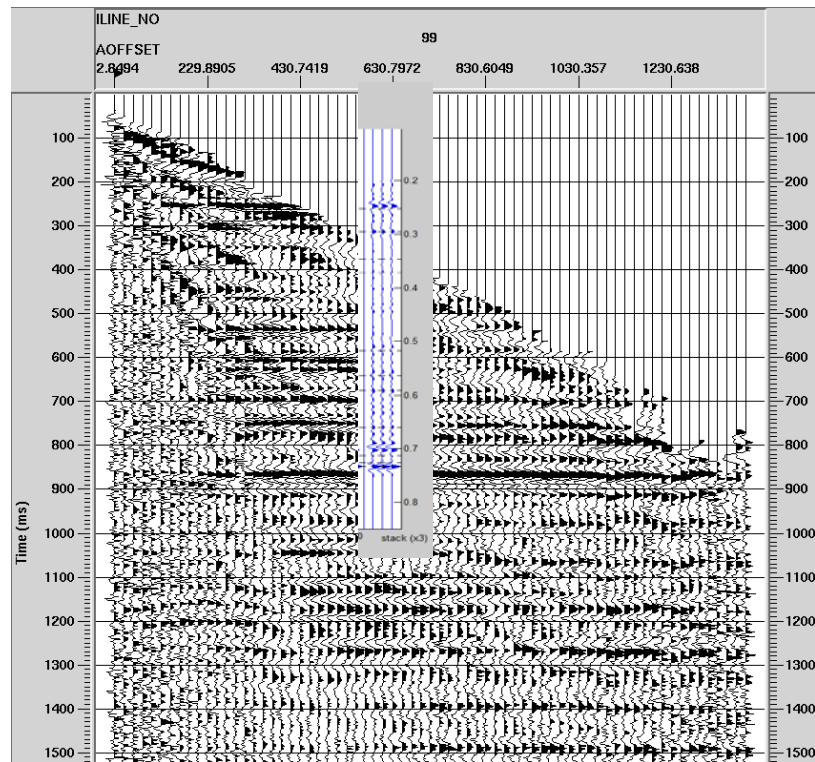


FIG.11. Common offset gather with NMO and static correction for the 3D-3C real data (Helen Isaac). In the mid part, the synthetic seismogram for PP wave is compared with real section.

## 2D shot model

Fig.12 is a 2D geological and velocity model made by 3D seismic interpretation result and well log data. The recording pattern, on this section, is a single shot on the mid ( $x=500$  m) and 65 live geophones spread on a line with 15 m group interval. Modelling method is ray tracing as indicated in FIG.12.

Figures 13a and 13.b are synthetic shot records, and they result of using ray tracing method to make P wave reflection (13.a.) and P and S reflection and refraction events. A thin weathering layer is added to the model.

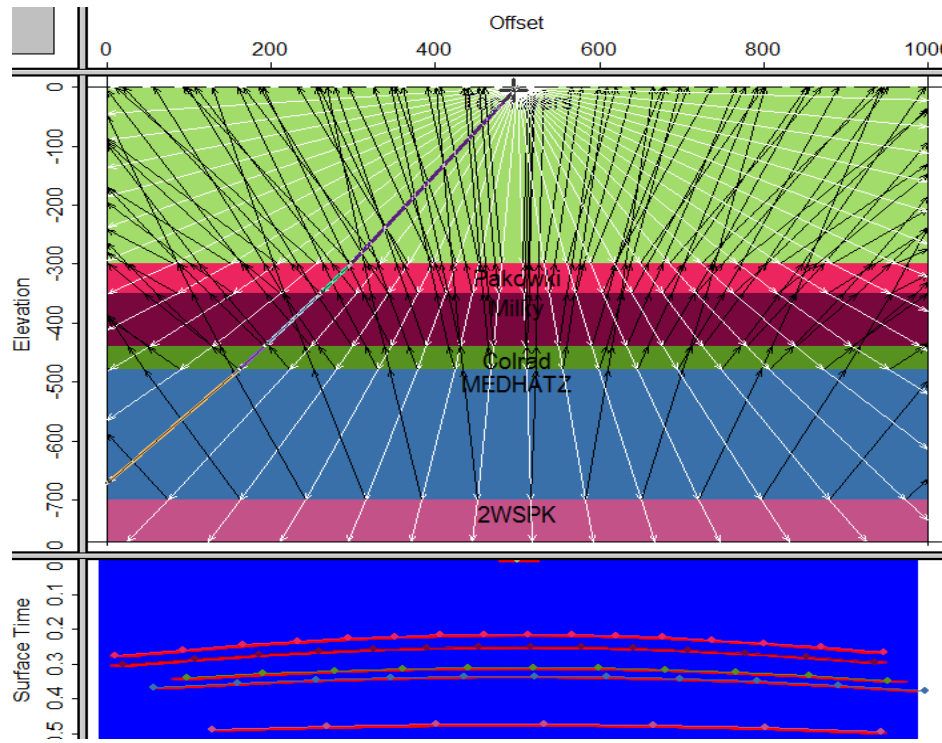


FIG.12. 2D geology and velocity model for the interest zone and ray tracing model and its result in time

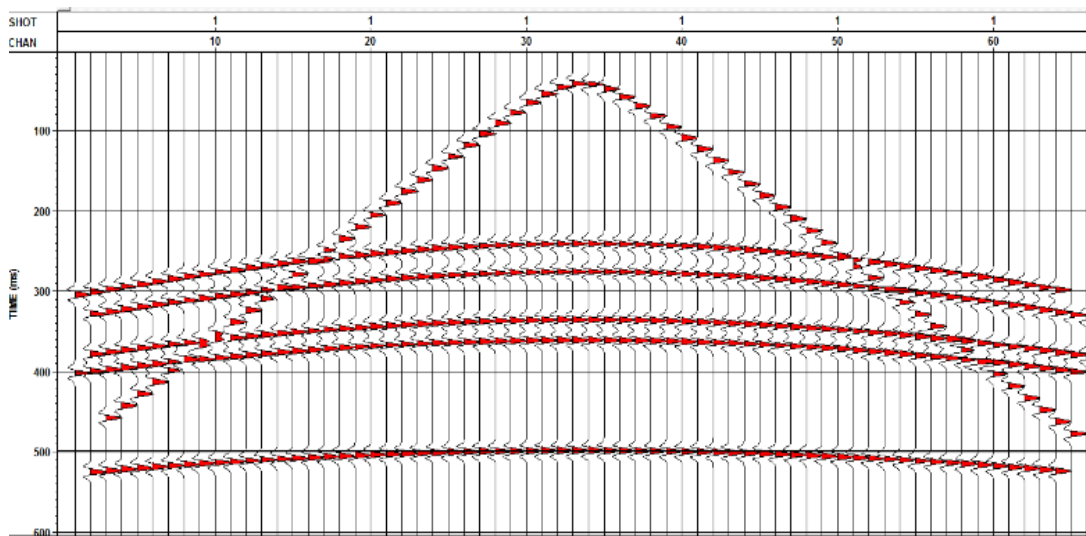


FIG.13a.synthetic shot record of P wave reflection wave. A thin weathering surface is considered for modelling.

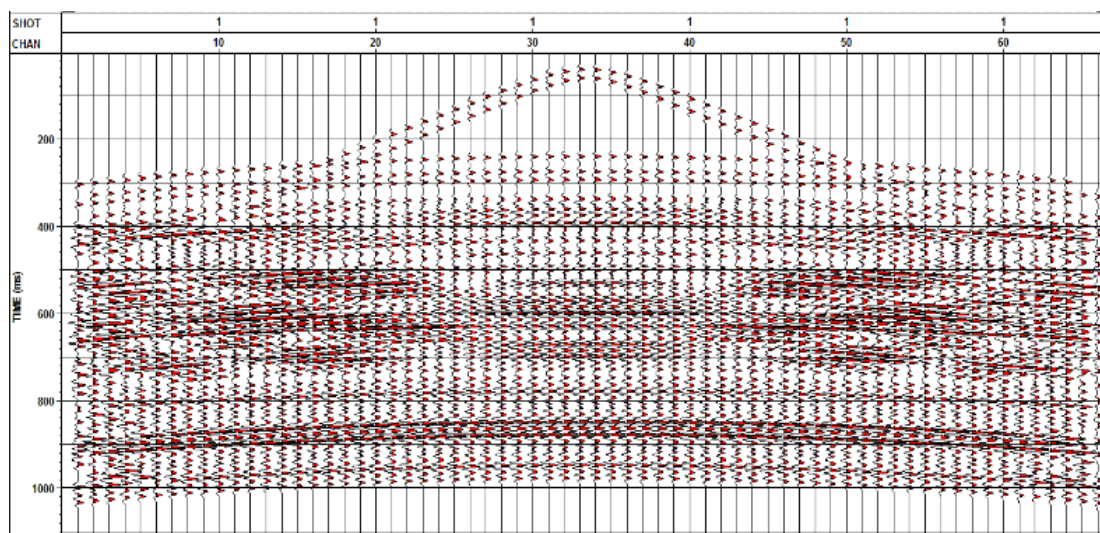


FIG.13b.Synthetic shot of full S and P wave reflections and refractions for the model with a thin weathering surface.This model has 1 km length , 65 live geophones and group interval is 15 m.

## SUGGESTED OPTIONS

### Option A

<b>Option A</b>		
<b>Parameters</b>	<b>Main</b>	<b>Mid core</b>
Bin size	5	5
Receiver interval	10	10
Receiver line interval	100	50
Shot interval	10	10
Shot line interval	100	50
Total Survey area	1000*1000	500*500
Maximum Offset	1407	
minimum offset	14	7
Largest minimum offset (LMOS)	134	64
Maximum fold	83	185
The highest fold (pp)	185	
Maximum inline offset	1000	
Maximum xline offset	1000	
Aspect ratio	100%	
Total shots	1600	
Total live geophones	1600	

Table 2. Designing parameters

Analysis and parameters calculation in the last sections, and necessity to have a semi high resolution seismic profile for the research purpose, lead us to suggest option A. For the design quality control, in the next pages, maps and diagrams designing attributes are prepared.

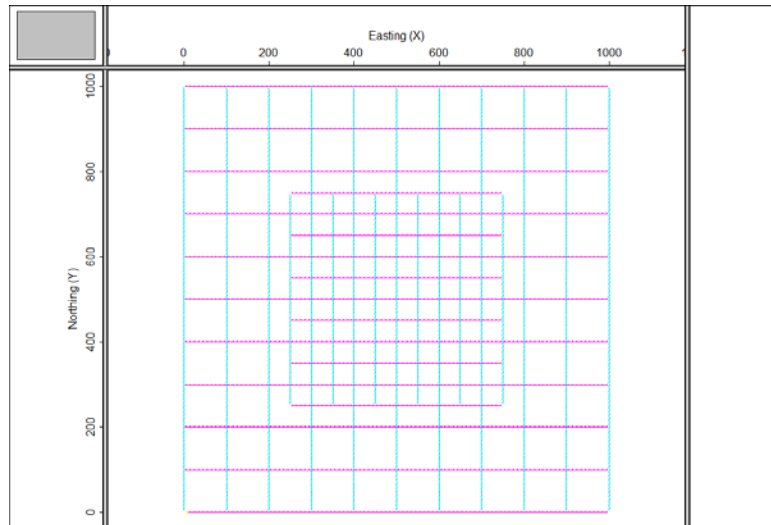


FIG.14. Acquisition geometry. The Blue and pink lines show receiver and shot lines.

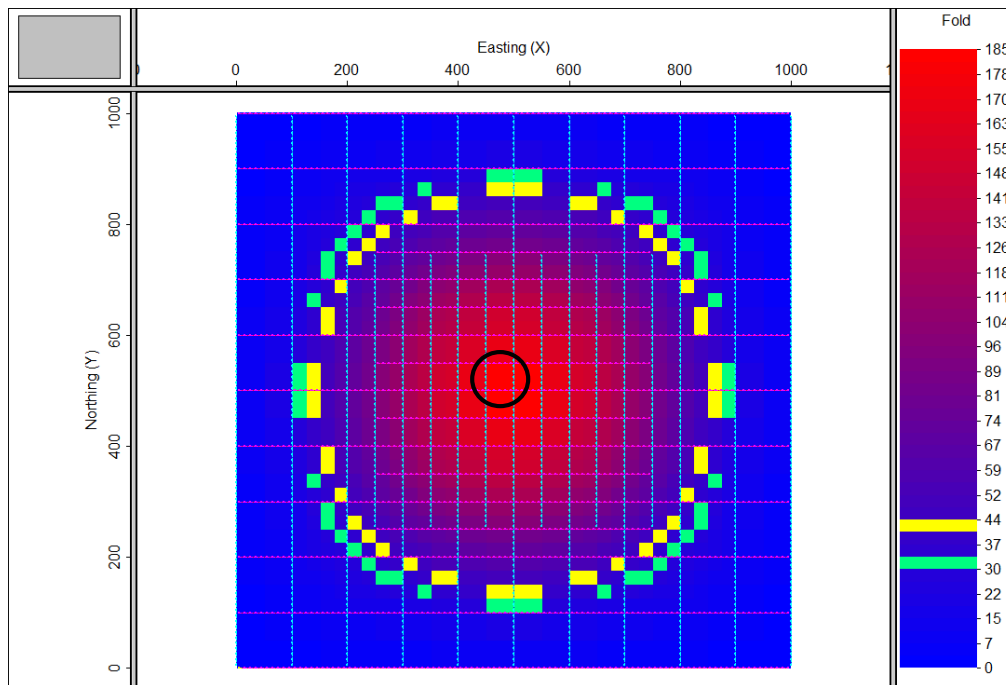


FIG.15. Fold map for option A. Fold more than 30 and 40 (inside the green and yellow circle) that cover about 50% and 42% and of acquisition area. In the internal core fold is from 55 to 185. The black circle indicates the area that is considered for azimuth and offset distribution study in the following figures.

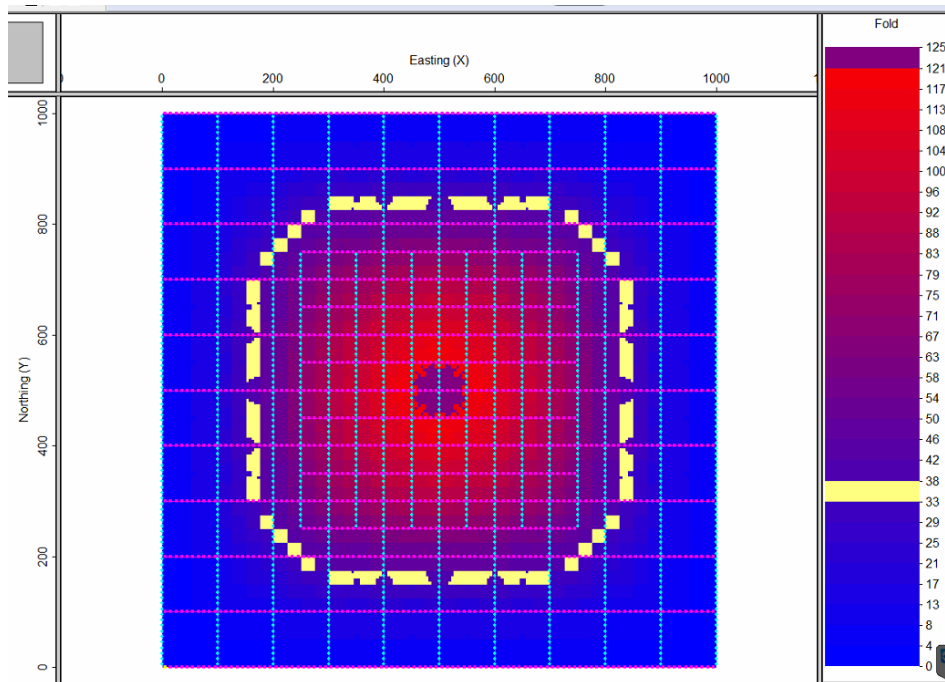


FIG.16. PP fold for offset 0-700 m

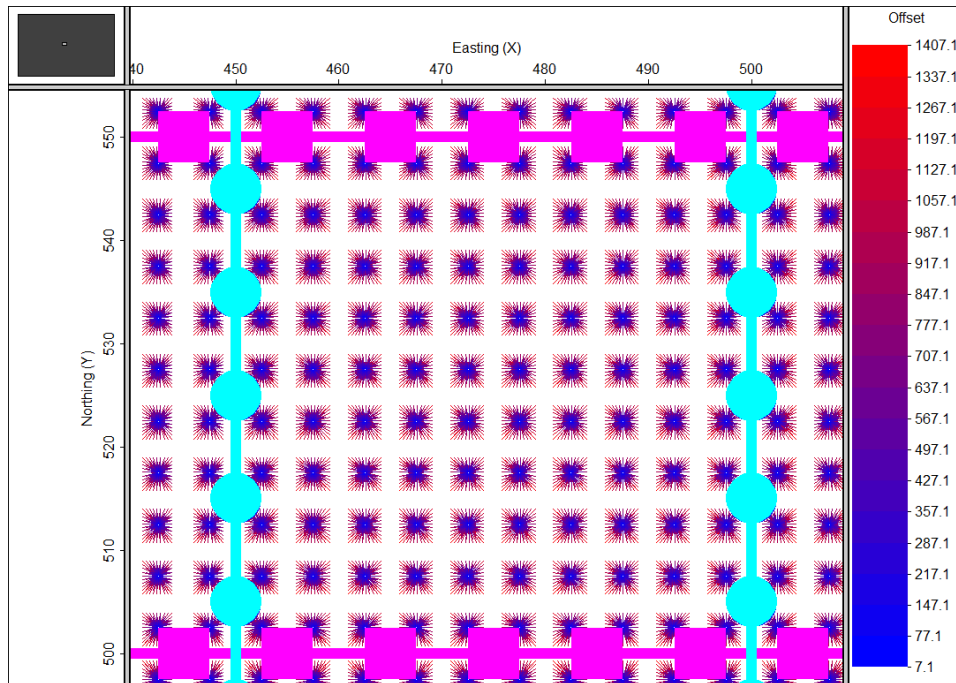


FIG.17. Azimuth distribution for whole offset ranges in the mid core (black circle in Fig.15)

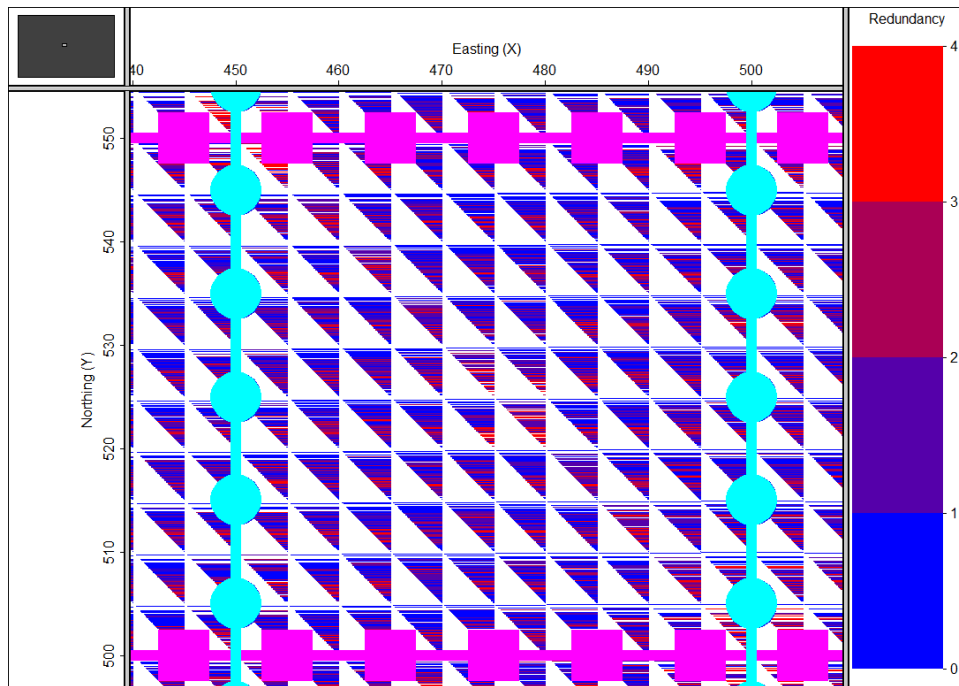


FIG.18. Whole offset distribution in the mid core (black circle in Fig.15)

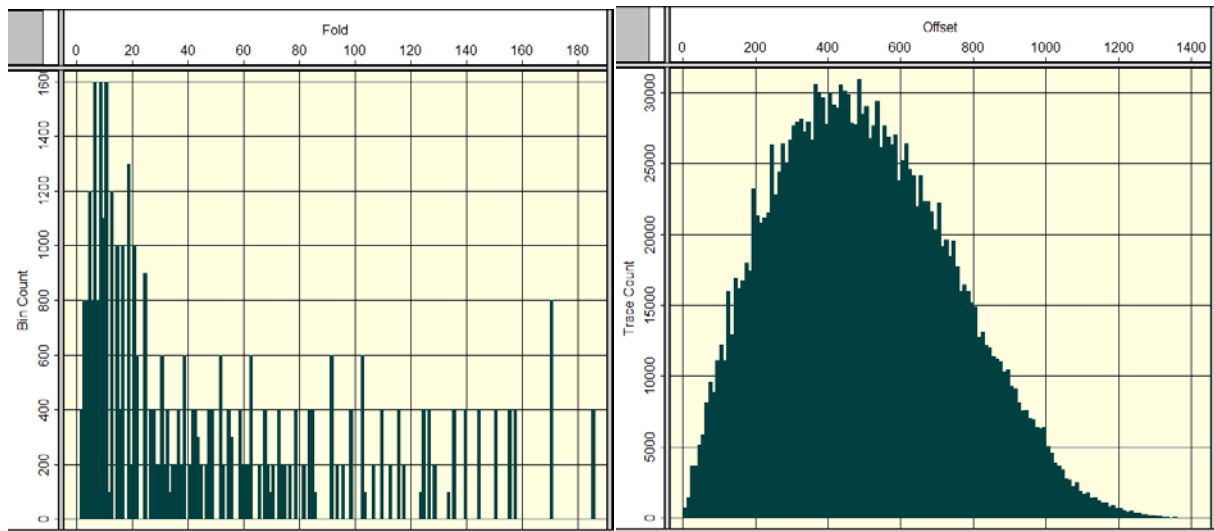


FIG.19. Left: Histogram of Fold, the numbers of bins that fall in each range of fold values  
 Right: Histogram of Offset, the number of traces that fall in each range of Offset values

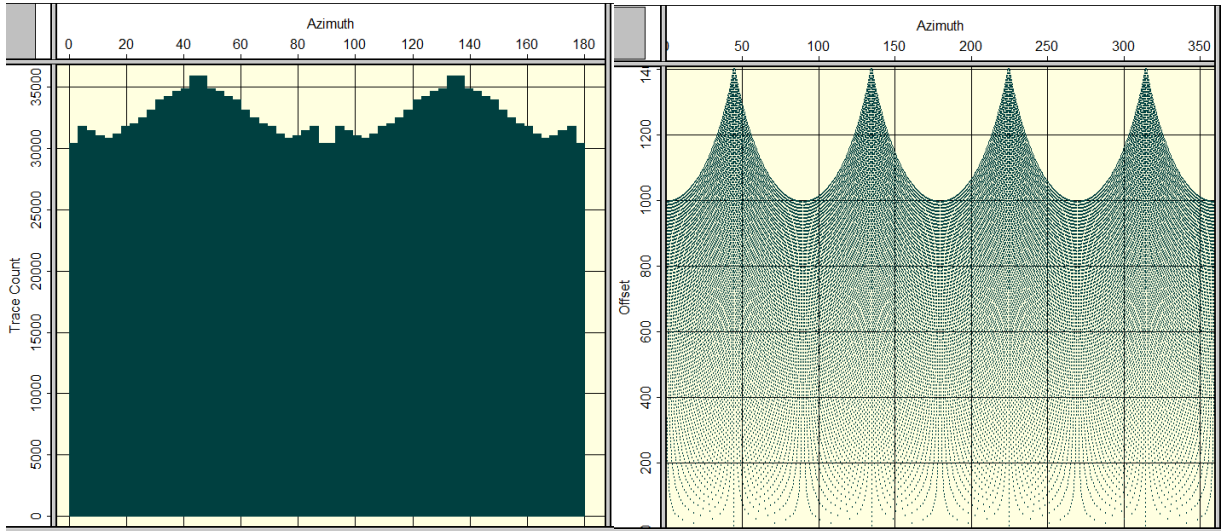


FIG.20. Left: Histogram of azimuth, the number of traces that fall in each range of azimuth values. Right: Offset versus azimuth, each trace at its (Azimuth, Offset) coordinates, and shows the relationship between the two values

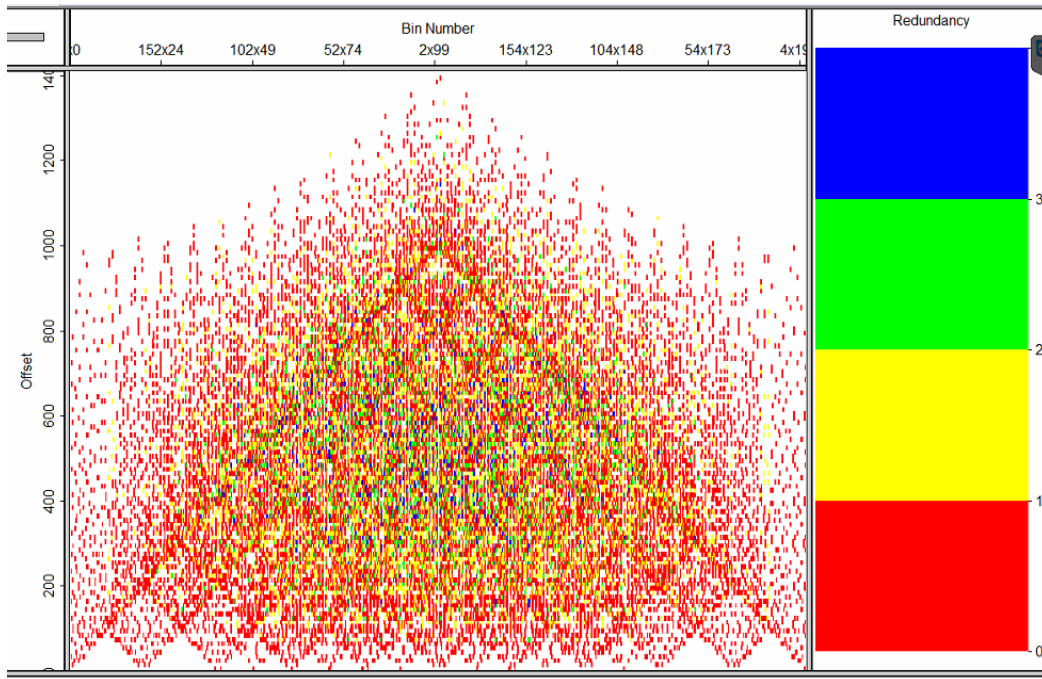


FIG.21. Offset redundancy, the number of traces that fall in each section; gaps indicate missing offset



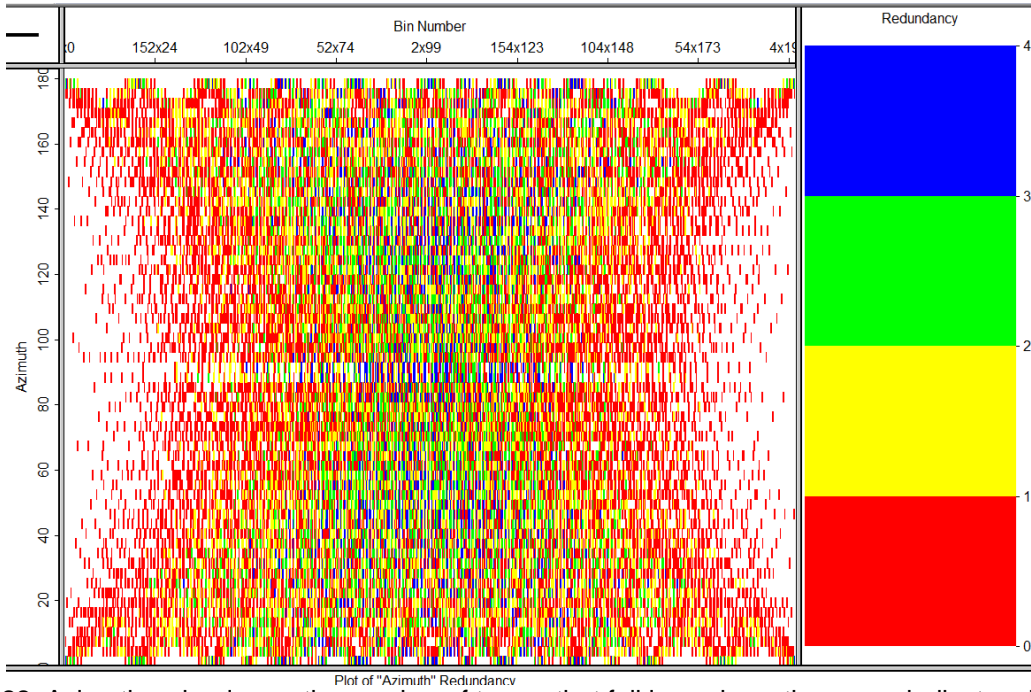


FIG.22. Azimuth redundancy, the number of traces that fall in each section; gaps indicate missing azimuth

*Results for PS designing*

The base of PS designing is concept of CCP, in this paper, non-asymptotic method is used for drawing fold map and calculating other attributes. The flat target is considered in 500 m depth.

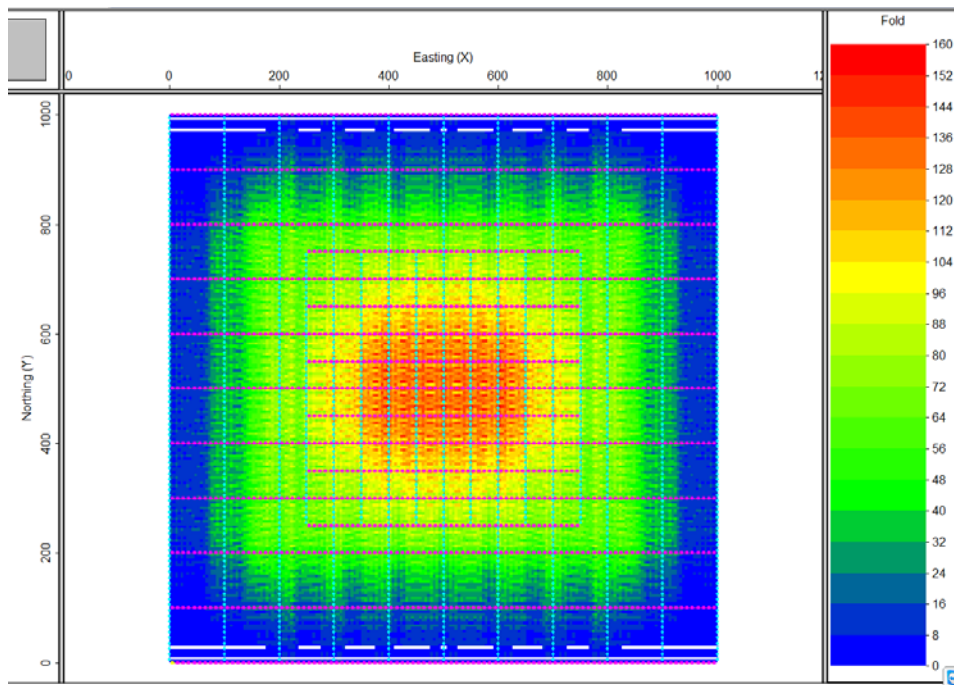


FIG.23.PS fold map for 500 m depth, (non-asymptotic method)

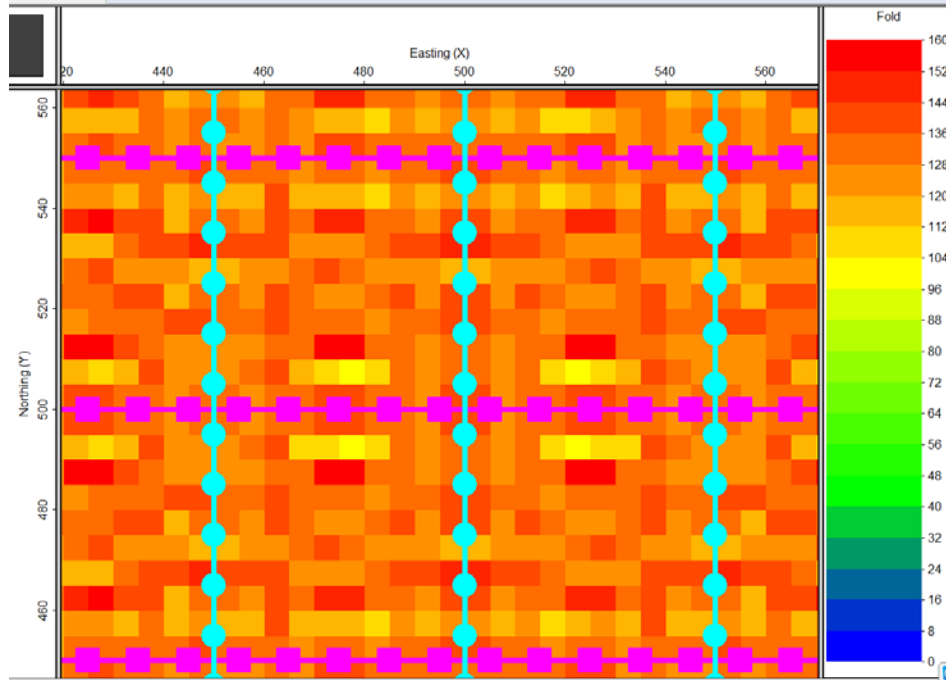


FIG.24.PS fold map for 500 m depth in the mid core

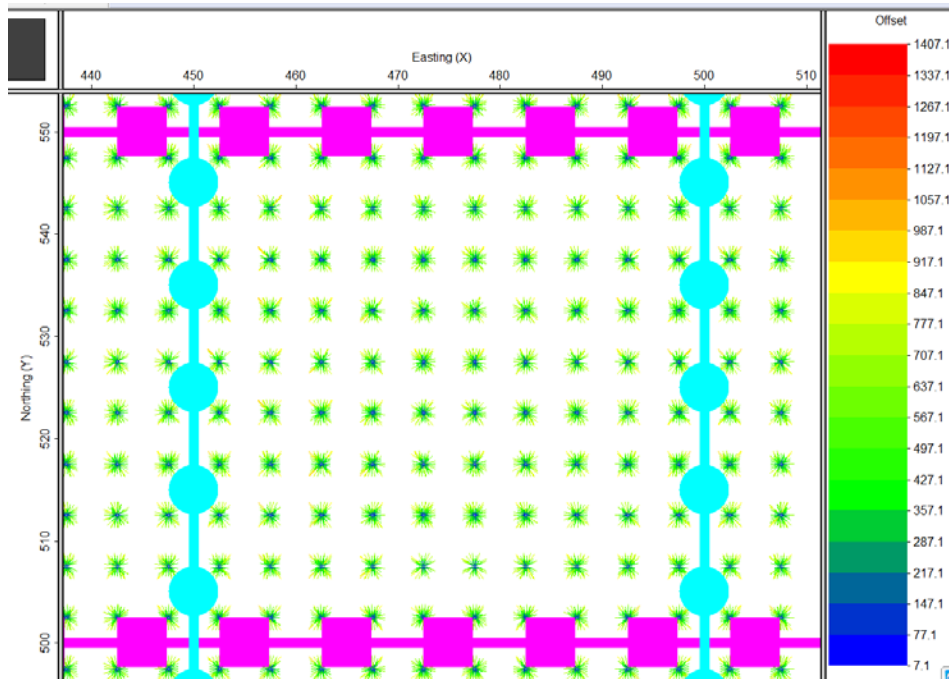


FIG.25. Azimuth distribution in the mid core for PS data

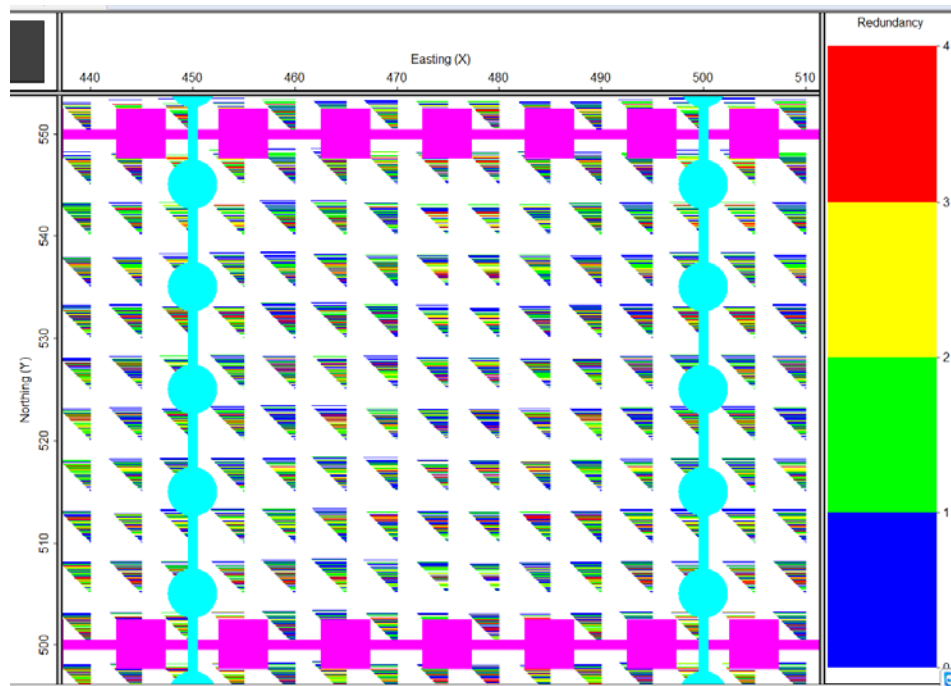


FIG.26. Offset distribution in the mid core for PS data

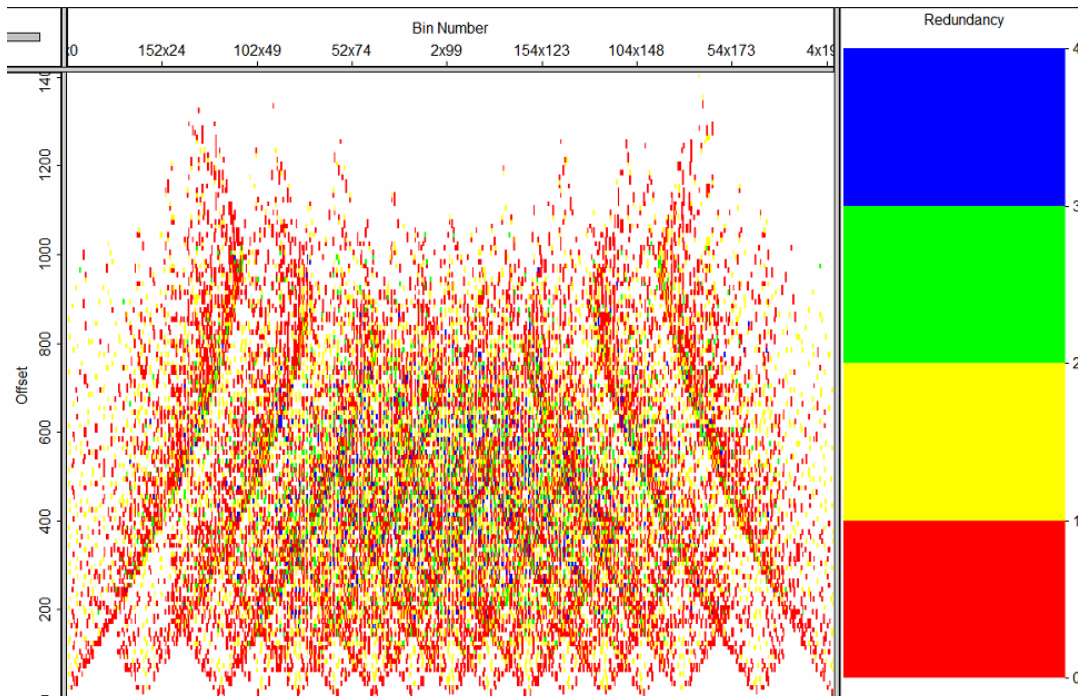


FIG.27. Offset redundancy for PS wave, the number of traces that fall in each section; gaps indicate missing offsets

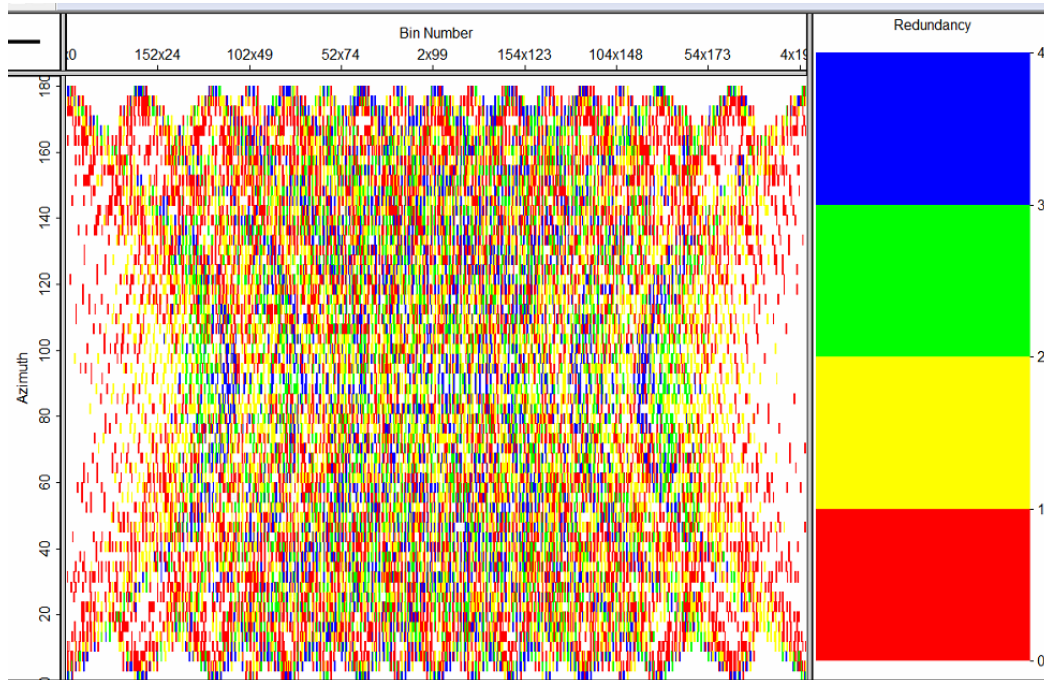


FIG.28. Azimuth redundancy for PS wave, the number of traces that fall in each section; gaps indicate missing azimuth

For the option A, fold is concentrated mainly in the mid core and fold map shows that just 50% of acquisition area will reach to the fold more than 30. Maximum nominal fold is 185 and the mid core high density acquisition zone guarantees high fold as >100 for the offset 0-700 m. Because aspect ratio is 100% and box and patch is symmetric, azimuth and offset distribution maps are perfect. Azimuth-offset histogram indicates a good coverage for offset less than 1 Km and 360 degree azimuth, (also there are lack of data for some azimuth in the offset higher than 1 Km, but this part is not in our interest zone).

The offset redundancy diagram as we expected, shows a zigzag pattern that is coming from orthogonal geometry. It shows a high redundancy for the offset 300-700m.

For the calculating PS fold, OMNI uses non-asymptotic PS conversion point between shot and receiver. It considers a flat target layer that is 500m for the project. PS fold and offset, azimuth distribution maps shows a suitable condition for the PS data acquisition.

## OPTION B

Option B is a simple designing pattern, with increasing bin size to 7.5 m and decreasing box size to 60\*75 m. It cause a higher fold and S/N for the whole area, but it can decrease resolution a little. Table 3. indicates parameters for the option B and fold maps, azimuth and offset distribution is shown in the following pages.

This option has 40% and 25% less shot and receiver points respectively. However, option B saves suitable fold distribution condition in the target zone.

<b>Option B</b>	
<b>Parameters</b>	
Bin size	7.5 m
Receiver interval	15 m
Receiver line interval	60 m
Shot interval	15 m
Shot line interval	75 m
Total Survey area	1020*975 m
Maximum Offset	1407 m
minimum offset	10.6 m
Largest minimum offset (LMOS)	85.5 m
Maximum fold	221
The highest fold (pp)	221
Maximum inline offset	1000
Maximum xline offset	1000
Aspect ratio	95.5%
Total shots	952
Total live geophones	1170

Table 3. Design parameters for the second option

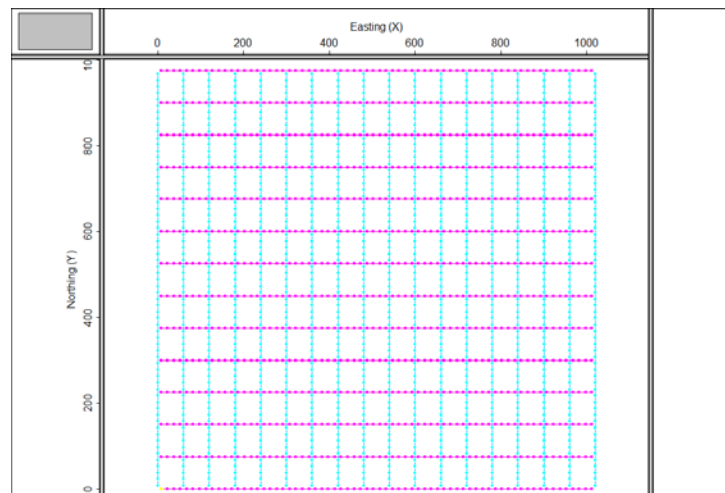


FIG.29.Lines geometry and revisers and shots position for the option B

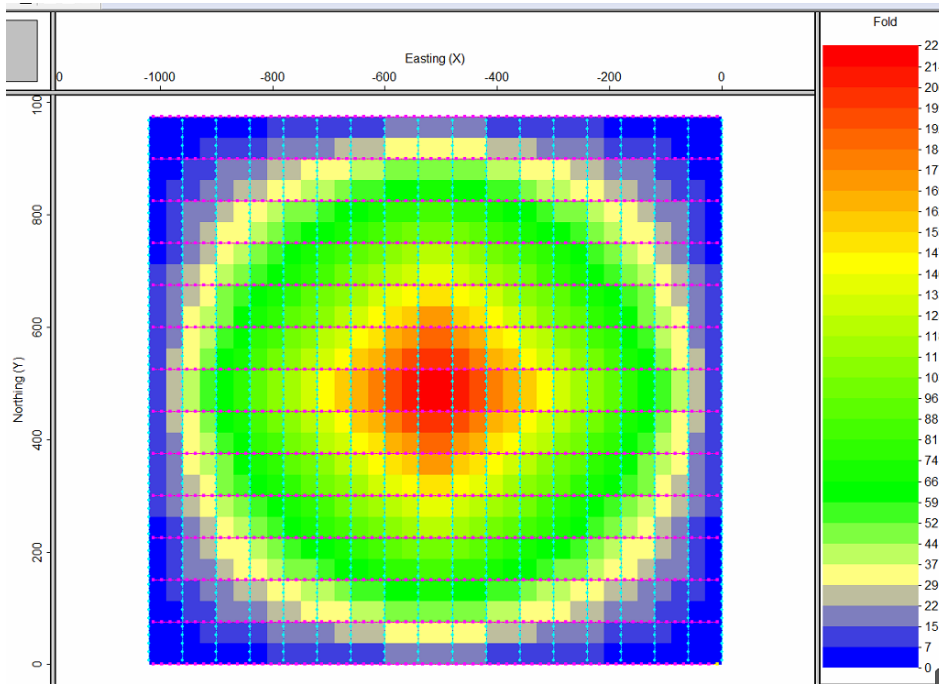


FIG.30. Fold map for option B. Fold more than 30 (inside the green and yellow circle),so 66% of area has fold over 30.



FIG.31. Azimuth distribution in the highest fold box.

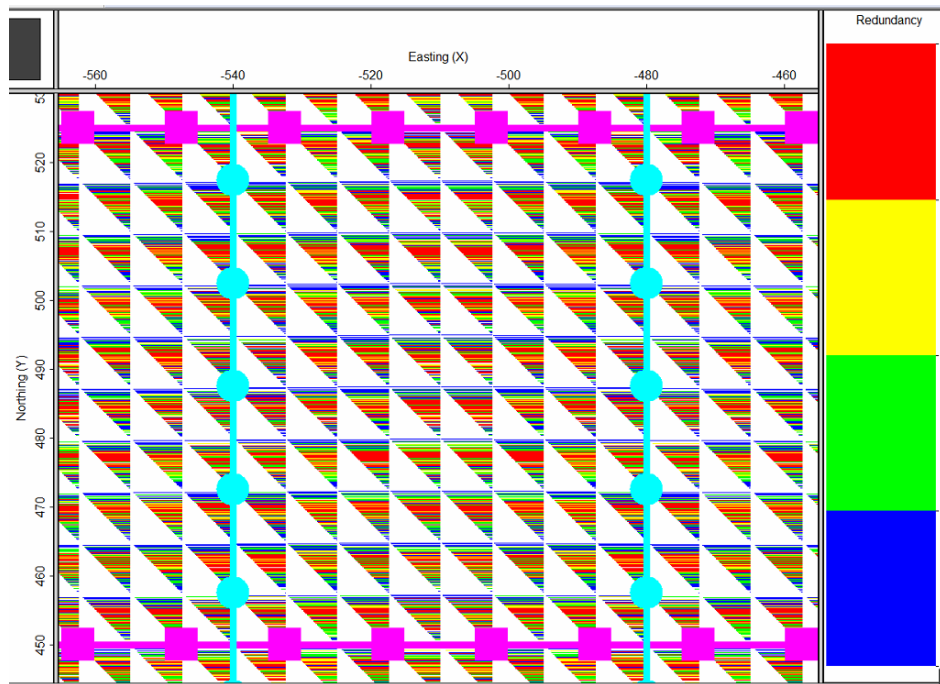


FIG.32. Offset distribution in the highest fold box.

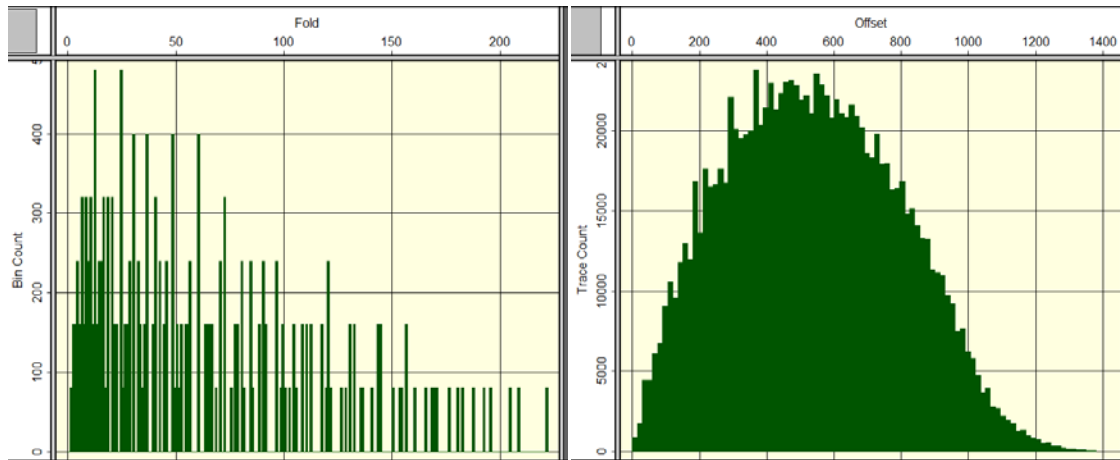


FIG.33. Left: Histogram of Fold, the numbers of bins that fall in each range of Fold values  
 Right: Histogram of Offset, the number of traces that fall in each range of Offset values

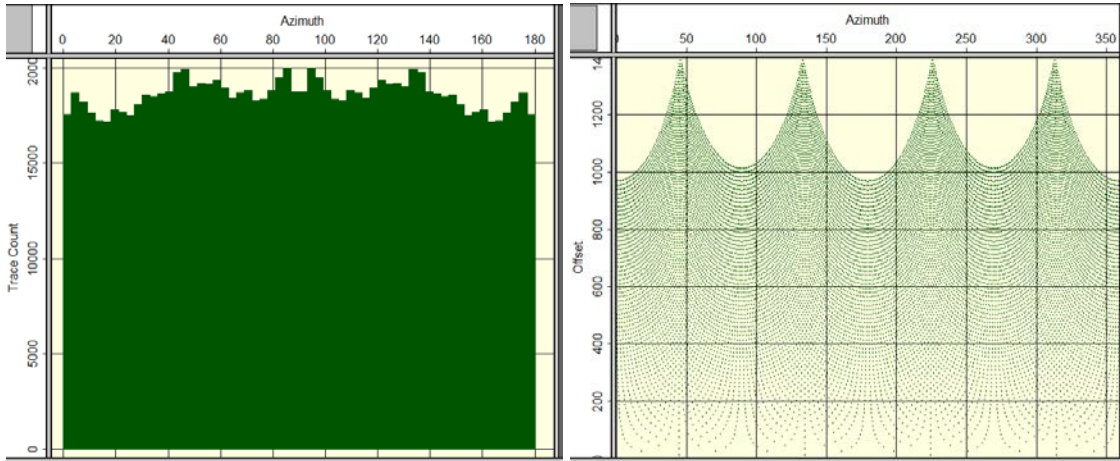


FIG.34. Left: Histogram of Azimuth, the number of traces that fall in each range of Azimuth values. Left :Offset versus Azimuth, each trace at its (Azimuth, Offset) coordinates, and shows the relationship between the two values

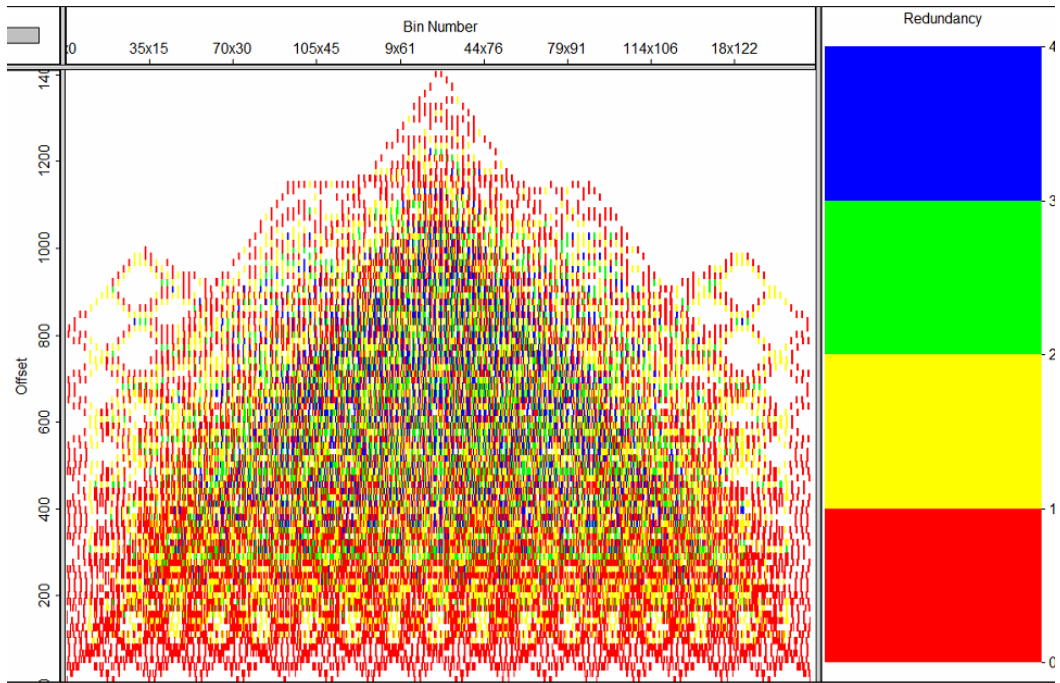


FIG.35. Offset redundancy, the number of traces that fall in each section,gaps indicate missing offset



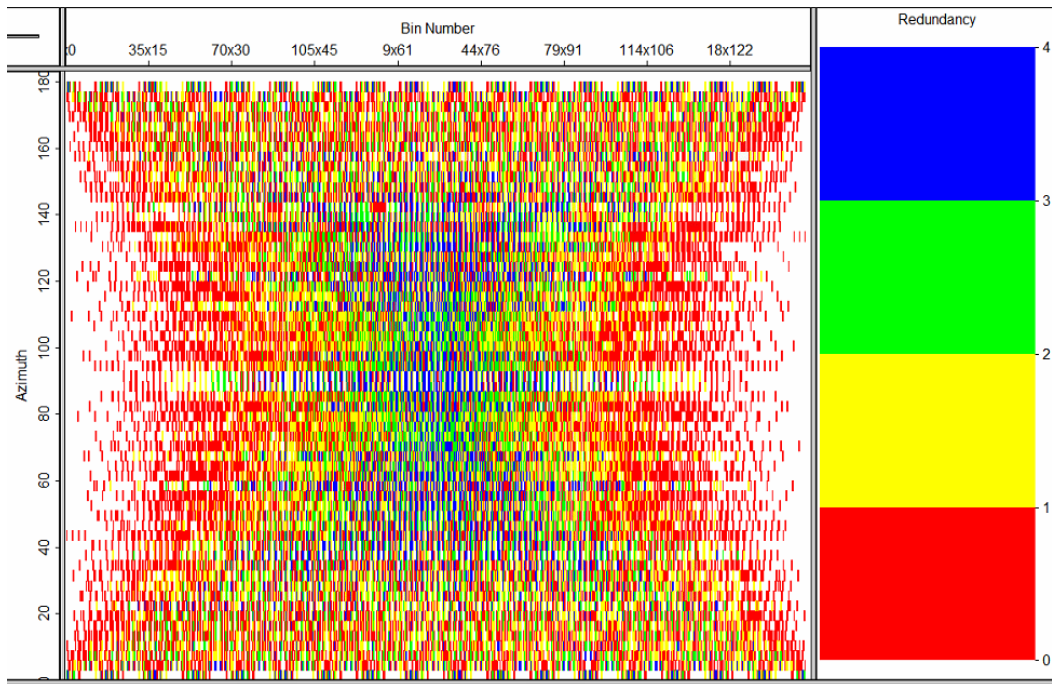


FIG.36. Azimuth redundancy, the number of traces that fall in each section; gaps indicate missing azimuths

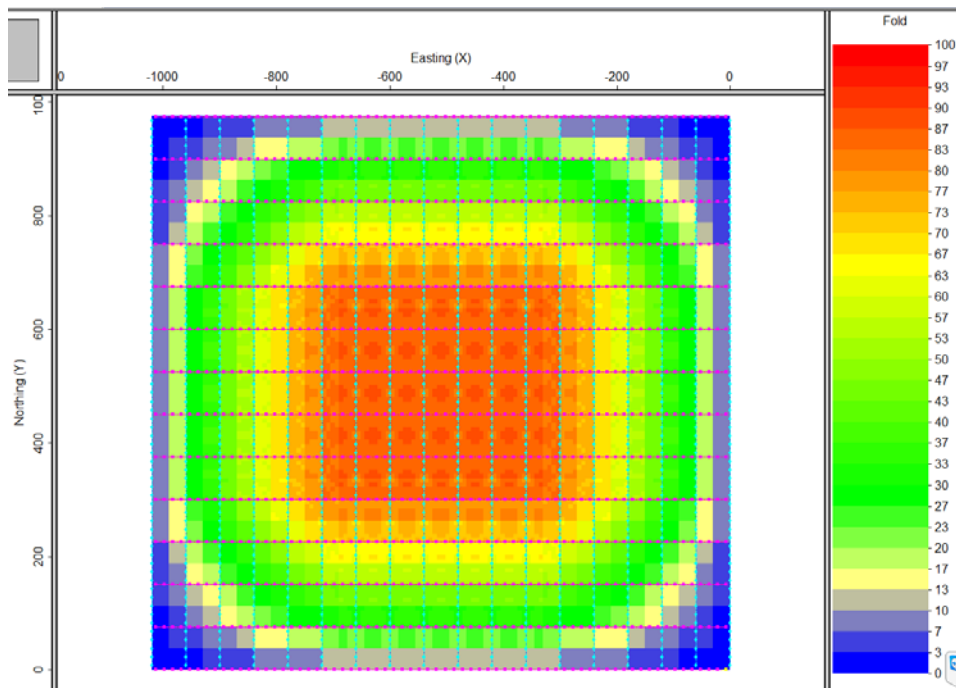


FIG.37. Fold map for offset 0-700m (in the target range)

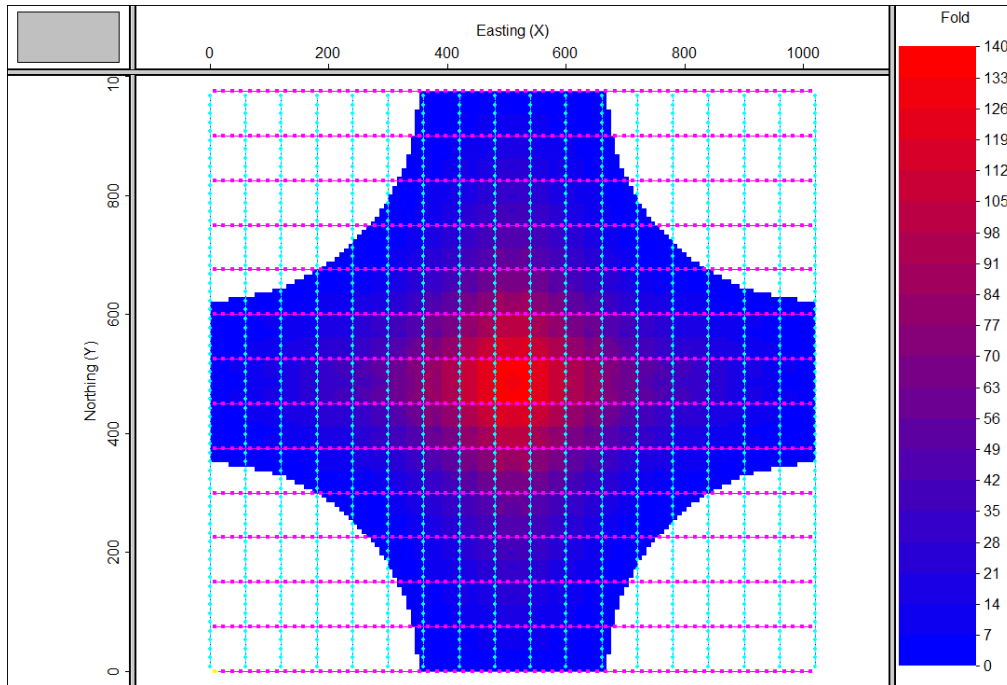


FIG.38. Fold map in the long offset between 700-1400 m

*Results for PS design*

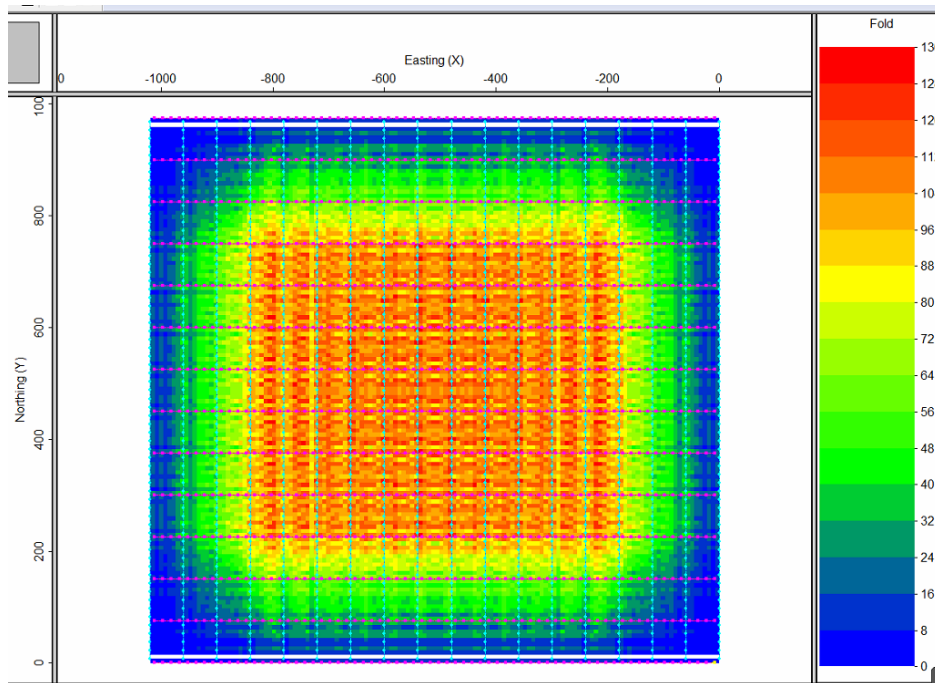


FIG.39. PS fold for the target in 500 m depth (non-asymptotic conversion points).

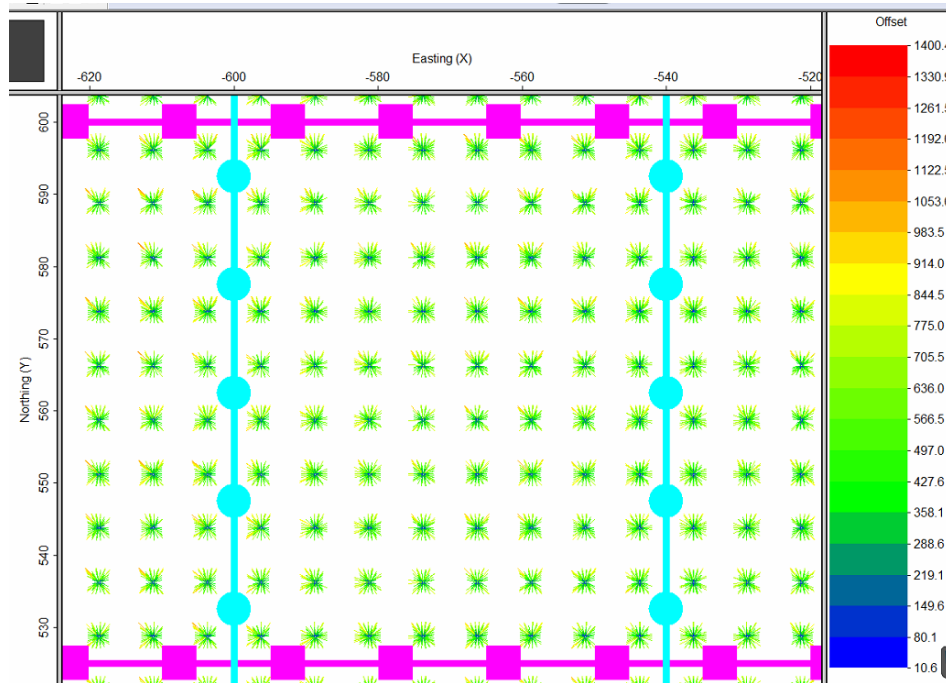


FIG.40. Azimuth's spider diagram

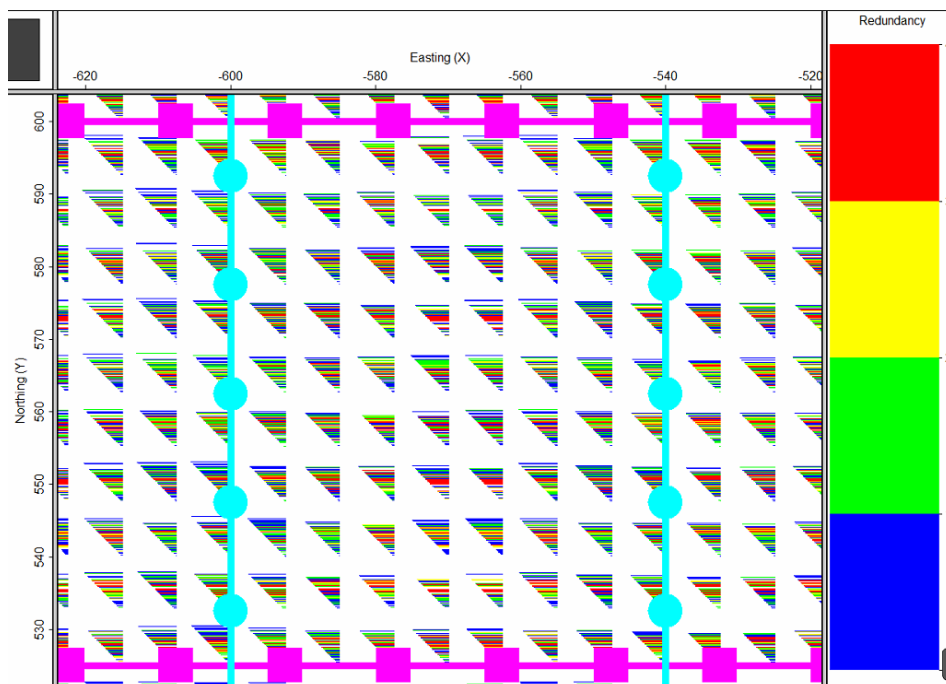


FIG.41. Offset distribution diagram

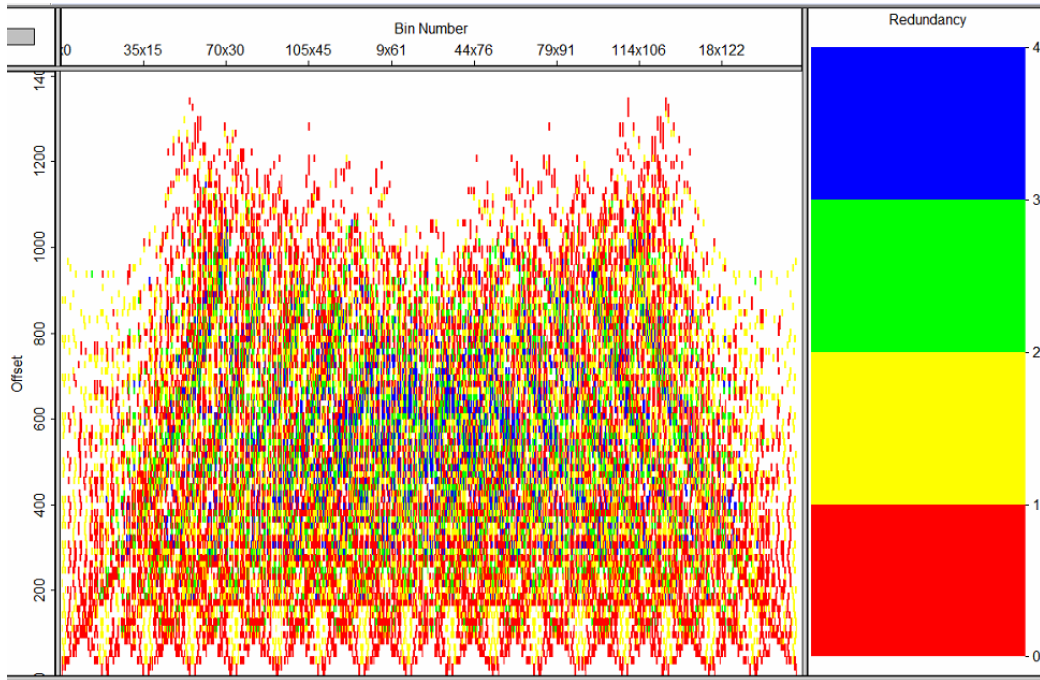


FIG.42. Offset redundancy for PS wave, the number of traces that fall in each section,gaps indicate missing offset

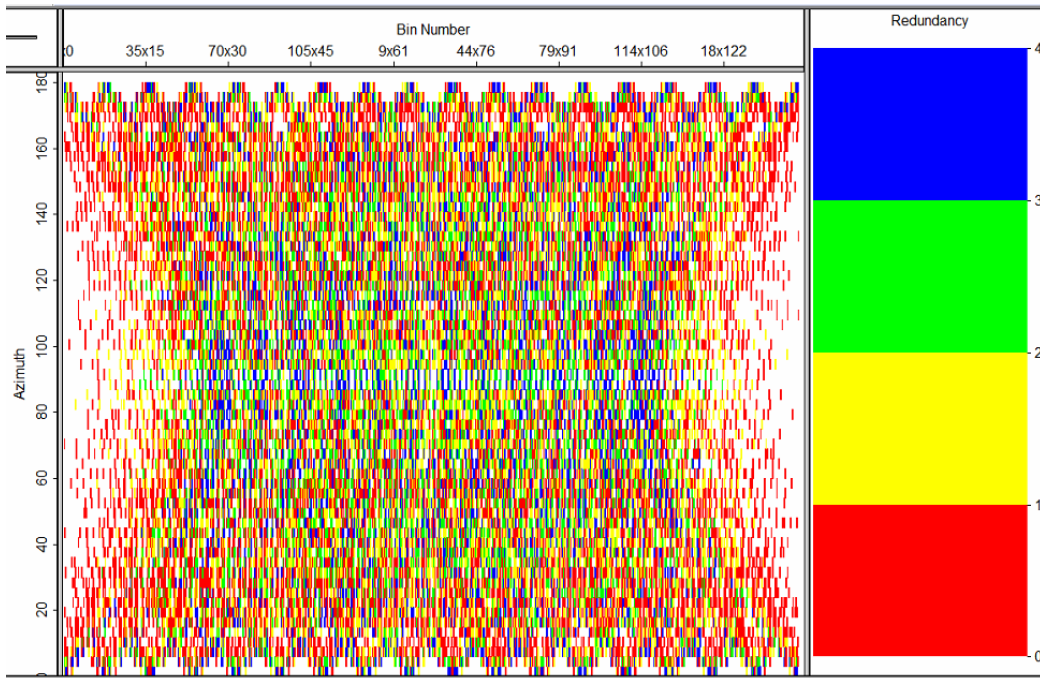


FIG.43. Azimuth redundancy for PS wave, the number of traces that fall in each section,gaps indicate missing azimuth

## CONCLUSIONS

The project area is a flat surface and subsurface zone, with no complex geology condition. As mentioned, the project is a limited CO<sub>2</sub> injection test with small plume size, so acquisition area is 1\*1 Km. Parameters are selected for a semi high resolution acquisition. Two set of parameters as option A and B are introduced. Both have good and flawless coverage for offset and azimuth distribution for the PP acquisition.

The fold map condition for the option A shows a high fold range in the mid core (500\*500m). For the second option, fold map is spread constantly in the acquisition area and can make a bigger image and data zone if injection plume grow during injection. With considering shot and receiver points, economically option B is a better choice as shot points are 40% less than first option, especially high fold contents are supported by reservoir points more than source points. However option A has better resolution because of smaller bin size.

## ACKNOWLEDGMENTS

We would like to thanks CREWES Sponsors for their support, and GEDCO (Schlumberger) for providing design software (OMNI). We also gratefully acknowledge support from NSERC (Natural Science and Engineering Research Council of Canada) through the grant CRDPJ 379744-08.

## REFERENCES

- Cordson, A., Galbraith, M., and Peirce, J., 2000, Planning land 3-D seismic surveys, Soc. Expl. Geophys., Tulsa, Oklahoma.
- Evans, B. J., 1997, A handbook for seismic data acquisition: Soc. Expl. Geophys., Tulsa, Oklahoma.
- Liner, C. L., and Gobeli, R., 1996, Bin size and linear v(z): 67th Ann. Internat. Mtg., Soc. Expl. Geophys., Expanded Abstracts, 43-46.
- Liner, C. L., and Gobeli, R., 1997, 3-D seismic survey design and linear V(z): 67th Ann. Internat. Mtg., Soc. Expl. Geophys., Expanded Abstracts, 43-46.
- Liner, C. L., Gobeli, R., and Underwood, W. D., 1997, Aspects of 3-D seismic survey design for linear v(z) media: 59th Mtg. Eur. Assoc. Expl. Geophys., Abstracts, Paper B002.
- Liner, C. L., Underwood, W. D., 1999, 3-D seismic survey design for linear V(z) media: Geophysics, 64, 486-493.
- Margrave, G. F., 1997, Seismic acquisition parameter considerations for a linear velocity medium: 67th Ann. Internat. Mtg., Soc. Expl. Geophys., Expanded Abstracts, 47-50.
- Pegah, E., Feiz Aghaei, B., Javaherian, A. R., and Nowroozi, D., Determination of Bin size and Migration aperture in 3-D seismic survey design for AHWAZ oil field with using linear velocity model (LVZ): EAGE, Expanded Abstract, First International Petroleum Conference & Exhibition, Shiraz, Iran, 4-6 May 2009.
- Stone, D.G., Designing Seismic Surveys in Two and Three Dimensions, 1994, SEG, Tulsa, Oklahoma.
- Telford, W. M., Geldart, L. P., and Sheriff, R. E., 1990, Applied geophysics, 2nd ed: Cambridge Univ. Press.
- Vermeer, G. J. O., 2002, 3-D seismic survey design, Soc. Expl. Geophys., Tulsa, Oklahoma.